Intensity of the Earth's magnetic field in Greece during the last five millennia: New data from Greek pottery

Intensity of the Earth's magnetic field in Greece during the last five millennia: New data from Greek pottery

Tema Evdokia[1], Gómez-Paccard Miriam[2], Kondopoulou Despina[3], Ylenia Almar[2]

[1]*Dipartimento di Scienze della Terra, Università degli Studi di Torino, via Valperga 35, 10125, Torino, Italy, evdokia.tema@unito.it*

[2]*Institut de Ciències de la Terra Jaume Almera, ICTJA-CSIC, Lluis Solé i Sabaris s/n, 08028, Barcelona, Spain, mgomezpaccard@ictja.csic.es, yalmar@ictja.csic.es*

[3]*Geophysical Laboratory, School of Geology, Aristotle University of Thessaloniki, 54124, Thessaloniki, Greece, despi@geo.auth.gr*

Abstract

New archaeointensity results have been obtained from the study of four ceramic collections coming from archaeological sites in Greece. The age of the ceramic fragments, based on archaeological constrains and radiocarbon analysis, range from 2200 BC to 565 AD. Low-field magnetic susceptibility versus temperature reveals a good thermal stability for most of the samples. However, for some samples the thermomagnetic curves are not reversible indicating mineralogical changes during heating. Isothermal remanent magnetization (IRM) acquisition curves and thermal demagnetization of three orthogonal IRM components have also been performed. The rock magnetic results identify magnetite and/ or Ti- magnetite as the main magnetic carriers in the studied samples. Classical Thellier experiments with regular partial thermoremanent magnetization (pTRM) checks have been conducted on 125 specimens belonging to 34 independent ceramic fragments. Only 61 archaeointensity determinations (at specimen level) that correspond to linear NRM-TRM plots were used for the calculation of the site mean archaeointensities. The effect of the anisotropy of the thermoremanent magnetization (TRM) and cooling rate upon TRM intensity acquisition have been investigated in all the specimens. The maximum difference between the TRM anisotropy corrected and uncorrected intensities is around 30% at specimen level confirming that the TRM effect can be very important

in ceramic samples. Cooling rate correction factors determined per specimen are up to 10% with only one exception that reaches 35%. Despite the moderate success rate of archaeointensity determination (around 50%) reliable mean site intensities have been obtained, with *in situ* intensities ranging from 53.6 ± 4.1 to 69.3 ± 3.9 μT, corresponding to virtual axial dipole moments from 9.2 ± 0.7 to 11.9 ± 0.7 x 10^{22} Am^2. The new data are reasonably consistent with other available data for the studied region as well as with the SV reference curves for Greece and the South Balkan Peninsula, and the regional and global geomagnetic field models results. Combined with previous published data from the area, they confirm that important changes of the Earth's magnetic field intensity occurred in Greece during the last five millennia. For some periods, the available archaeointensity data for the Balkan area show a large dispersion, even for data corresponding to high quality intensity standards, whereas for other periods their limited number prevents a reliable description of geomagnetic field intensity changes. This evidences the need of new reliable and well dated archaeointensity data in order to obtain a robust description of geomagnetic field intensity changes during the last five millennia in this area.

Keywords: Archaeomagnetism; Archaeointensity; Thellier method; Greece

1. Introduction

Archaeomagnetic data are an important source of information in order to retrieve the variations of the Earth's magnetic field during the past few millennia. During the last decades, a significant number of data has been produced and compiled in various datasets of regional (e.g., Schnepp et al., 2004; Gómez-Paccard et al., 2006a and 2008; Tema et al., 2006; Tema & Kondopoulou, 2011) and global coverage (Korte et al., 2005; Genevey et al., 2008; Donadini et al., 2009). These data have been used for the computation of secular variation (SV) curves for certain regions such as France (Gallet et al., 2002), Germany (Schnepp & Lanos, 2005), Italy (Tema et al., 2006), the Iberian Peninsula (Gómez-Paccard et al., 2006b; 2008), the Balkan Peninsula (Tema & Kondopoulou, 2011) and regional (Pavón-Carrasco et al., 2009; 2010) and global (Korte & Constable, 2005; Valet et al., 2008; Korte et al., 2009) geomagnetic field models. However, there are generally more directional than intensity data (Korte et al., 2005; Donadini et al., 2009). That is mainly because the

laboratory procedure necessary to determine the archaeointensities is more time-consuming compared to the directional protocols and several mechanisms can cause failure of the archaeointensity experiments. The repeated heatings of the specimens during the laboratory treatment often cause physico-chemical transformations that can change their TRM acquisition capacity. Other physical mechanisms as the influence of the anisotropy of the thermoremanent magnetization (TRM) and the cooling time dependence of the TRM intensity must also be investigated and these effects must be considered in order to obtain accurate archaeointensities.

Systematic archaeomagnetic studies in Greece were initiated around the 80's and contrary to the general situation in Europe, archaeointensity data are more abundant than directional data (De Marco, 2007; De Marco et al., 2008; Spatharas et al., 2011; Tema & Kondopoulou, 2011). However, the quality of some of the Greek archaeointensity results has often been disputable. De Marco et al. (2008) have compiled a database including all available intensity data from Greece. They noticed a large dispersion, especially during the first millennium BC, where the majority of the data are concentrated. Following Chauvin et al. (2000) these authors also evaluated the Greek data and assigned a weighting factor in order to discriminate the variable reliability of the Greek archaeointensity data. A reference SV curve for Greece calculated by Bayesian modelling and covering the last seven millennia has also been proposed (De Marco et al., 2008). In a recent study, Tema & Kondopoulou (2011) have studied the SV of the geomagnetic field in the Southern Balkan Peninsula and they also observed a large scatter in their intensity data compilation. Even though the reasons for such scatter are not clear, the subjective interpretations of the Arai diagrams, the different laboratory protocols used by the different research groups, the often low number of specimens analysed per site, the often missing TRM anisotropy and cooling rate corrections and/or dating errors could be some of the possible causes (Chauvin et al., 2002; Donadini et al., 2009; Tema & Kondopoulou, 2011). On the other hand, the study of seven contemporaneous kilns excavated in Murcia (Gómez-Paccard et al., 2006c) where exactly the same archaeointensity protocol has been used, suggests that probably there is a precision limit linked to the experimental archeointensity procedure even for studies which follow the most high quality procedures. The acquisition of new, well-dated, high quality archaeointensity data is therefore crucial to obtain a reliable geomagnetic field intensity evolution. Well dated

high-quality data can also be used as reference points for assessment of the reliability of older data.

We present here new archaeointensity results from a collection of Greek ceramics that come from four different archaeological sites with ages ranging from 2200 BC to 565 AD. Archaeointensity experiments were performed at Torino and Barcelona Palaeomagnetic laboratories by splitting the samples and sharing the same experimental protocols. The new absolute archaeointensity data are based on several archeointensity determinations per ceramic fragment and per site and were obtained using the Thellier classical method (Thellier & Thellier 1959) with regular partial thermoremanent magnetization (pTRM) checks. The effect of TRM anisotropy and cooling rate upon TRM acquisition has been investigated in all the specimens. Therefore, the new data can be considered as reliable markers of past geomagnetic field intensity in Greece. Finally, the new intensities are compared with previously published data from Greece and nearby countries as well as with the SV curves available for Greece and the South Balkan Peninsula and the regional and global geomagnetic field models results.

2. Archaeological context and samples description

The ceramic fragments studied come from the archaeological sites of Archontiko (ARH), Skala Sotiros (SKS) and Tempi (TEM) situated at Northern and Central Greece and from the archaeological site of Paroikia (PAR), in Paros island (Fig. 1). Sites description, from the most recent to the older, is as follows:

TEMPI (TEM). During 2008 extended excavations were carried out in parallel with public works along the axis of the Tempi valley in Central Greece. Close to the tunnels of Kissavos mountain, remains of palaeochristian period were unearthed. Among them, a small part of a cemetery and few buildings, mostly artisanal, hosted several ceramic products. An orthogonal kiln, well preserved, and traces of a second one, provided the various types of collected fragments. The settlement was developed in two habitation phases: during the 4^{th} and the 6^{th} centuries AD, with important coin collections supporting these chronologies. Nevertheless, all ceramics found are dated from 518 to 565 AD, at the emperor's Justinian reign (Sdrolia, 2009). From this collection 9 independent ceramic fragments were collected.

PAROS (PAR). A Late Hellenistic-Early Roman ceramic workshop was excavated at Paroikia (Hasaki, 2004), hosting six ceramic kilns which operated between the 1^{st}

century BC and 1st century AD. Their last use is dated to the early imperial period on the basis of stratigraphy, kilns' type and ceramic characteristics. The workshop's production was primarily utilitarian. Four out of the six kilns have been archaeomagnetically sampled and the full geomagnetic field vector results of one kiln (PAR1) have been published by now (De Marco, 2007; De Marco et al., 2008). In the present study, pottery fragments from inside the workshop as well as from the auxiliary depository situated on the opposite side of the workshop, have been collected and studied. In the depository area, a collection of sherds and pottery were found and their contemporaneous date and close relation to the kilns is confirmed by archaeological evidence (Hasaki 2005, personal communication). The studied collection comprises 10 independent ceramic fragments, 8 coming from the kilns (PRCA) and 2 from the depository (PRCB).

SKALA SOTIROS (SKS)-Island of Thasos. The prehistoric settlement of Skala Sotiros, situated at the western part of Thasos island, has been systematically excavated between 1986 and 1991 by the IH' Ephorate of Prehistoric and Classical Antiquities at Kavala (Koukouli-Chrysanthaki, 1989) and was classified as Early Bronze age. Two habitation phases were unearthed, separated by a destruction level. Radiocarbon analysis on three coal samples gave ^{14}C ages as follows: 1. 3867±63 BP, calibrated at 68% 2464-2210 BC; 2. 3845±37 BP, calibrated at 68% 2453-2281 BC; 3. 3802±39 BP, calibrated at 68% 2322-2147 BC (Koukouli- Chrysanthaki, 1990). Additional radiocarbon results on two animal bones (Koukouli- Chrysanthaki, 2011 personal communication) give ages: 4. 3703±30 BP, calibrated at 68% 2140-2030 BC and 5. 3595±30 BP, calibrated at 68% 2015-1905 BC. The observed scatter of ages in quite important, nevertheless the site habitation was continuous and time limits between different phases difficult to set. The archaeologists consider as upper limit of the habitation the 2500 BC and lower limit 1900 BC. Given that the studied samples come from the younger phase, this allows a safe dating between 2200-2000 BC (Koukouli- Chrysanthaki, 2011 personal communication) and an age of 2100-2200 BC can be considered representative for our samples. A set of 6 independent pottery fragments were collected from this site.

ARHONTIKO (ARH). The ancient city of Arhontiko is located on a trapezoidal mound at the edge of the homonymous village, 4 km away from the ancient town of Pella. Since 1991, the Department of Archaeology of the Aristotle University of Thessaloniki, is excavating systematically the site, revealing a settlement with

successive phases between the end of Early Bronze age and the beginning of the Middle Bronze age. Several radiocarbon studies were performed, determining the oldest and main phases of the settlement from 2300 BC to 1900 BC (Maniatis et al., 2002). The ceramic collection used for the present study comes from the youngest excavated up to now habitation horizon I, phase A, and has been studied in the context of a Master Thesis (Deliopoulos, 2007). Radiochronological analysis of one sample, dates this phase more precisely at 1516-1414 BC (Papadopoulou, 2002), thus at the Late Bronze age. The up to now evaluation of the ceramics favours rather a 15^{th} century BC age. A total of 9 independent ceramic samples from this site have been collected and studied.

3. Magnetic mineralogy

Magnetic mineralogy experiments have been done at the ALP Palaeomagnetic laboratory (Peveragno, Italy), the Palaeomagnetic laboratory of Thessaloniki (Greece) and the Centre de Physique du Globe of the Royal Meteorological Institute (Dourbes, Belgium). Low-field magnetic susceptibility versus temperature experiments, isothermal remanent magnetization (IRM) acquisition curves and thermal demagnetization of three orthogonal IRM components (Lowrie, 1990) have been used for the evaluation of the thermal stability of the samples and the identification of the main magnetic minerals. The temperature dependence of low-field magnetic susceptibility from ambient temperature up to 700 ^{o}C was monitored using a Bartington MS2B susceptibility meter in combination with a MS2WF heating unit. Thermomagnetic curves are useful indicators for the thermal stability of baked materials and thus for the suitability of the material for archaeointensity studies. For Paros and Tempi the obtained heating and cooling curves are reasonably reversible (Fig. 2 b and d) indicating that no important mineralogical changes took place during heating. On the contrary, for some samples from Archontiko and Skala Sotiros the thermomagnetic curves show no reversible behaviour (e.g., Fig. 2 a and c) indicating mineralogical transformations during heating.

The IRM of representative samples was investigated at the ALP Palaeomagnetic laboratory (sites PAROS and TEMPI) using an ASC pulse magnetizer for imparting the IRM and a JR6 spinner magnetometer (AGICO) for measuring the remanence, and at the Dourbes Palaeomagnetic laboratory (sites ARH

and SKS) using a 2G Enterprises impulse magnetizer (model 66) for imparting the IRM and a 760 model SQUID cryogenic magnetometer (2G Enterprises) for remanence measurements. Stepwise magnetic fields up to 2 T were applied. Samples from all sites show almost similar magnetic properties. The IRM curves indicate that the saturation of the magnetization is generally reached at low fields varying from 0.2 to 0.4 T indicating the presence of a low-coercivity mineral such as magnetite (Fig. 3). Only few samples from Paros (e.g., sample PRCA-1, Fig. 3a) remain unsaturated after 1.6 T peak field and probably contain some minor high-coercivity mineral, most probably hematite. Thermal demagnetization of the three IRM components (Lowrie, 1990) induced along the three sample axes, applying first the maximum field (1.3 T) along Z-axis, then the intermediate field (0.5 T) along the Y-axis and finally the minimum field (0.1 T) along the X-axis, shows the dominating role of the magnetically soft fraction (< 0.1 T) with unblocking temperatures ranging between 480 and 560 ^{o}C (Fig. 4). These results point to magnetite or Ti-magnetite as the main magnetic carrier in the studied samples.

4. Archaeointensity analysis

Between four to six specimens per ceramic fragment were prepared for archaeointensity experiments. When possible, cubic specimens of 2 cm side were prepared directly. For the remaining material, specimens of about 1 cm x 1 cm and variable heights were cut and packed into salt pellets (following Rodriguez-Ceja *et al*., 2009) of about 2 cm side. Archaeointensity experiments were conducted at the Palaeomagnetic Laboratories of Peveragno (Italy) and the Institute of Earth Sciences Jaume Almera (UB-CSIC) in Barcelona (Spain). A total of 125 specimens coming from 34 independent ceramic fragments were measured. The thermal treatment was conducted using a MMTD-80 (Magnetic Measurements) and a TD-48 (ASC) oven. Remanent magnetization was measured using a JR6 spinner magnetometer (AGICO) and a SRM755R (2G Enterprises) three axes cryogenic superconducting rock magnetometer. The original Thellier method (Thellier & Thellier, 1959) with regular partial thermoremanent magnetization (pTRM) checks was used to estimate archaeointensities. Samples were heated from 100 ºC to temperatures at which more than 85% of the initial magnetization was lost. Between 8 and 19 temperature steps from room temperature up to 590 ºC were needed. Experiments were made in air and

a laboratory field of 60 μT was applied. At each temperature step, specimens were first heated and cooled with the laboratory field applied along the Z-axis of the samples and successively a new heating- cooling circle was repeated setting the laboratory field in the opposite sense. Every two temperature steps a pTRM check was performed in order to detect any change in the TRM acquisition capacity. TRM anisotropy and cooling rate dependence upon TRM intensity were taken into account to correct the archaeointensities. The TRM anisotropy tensor has been calculated for each specimen from the acquisition of a TRM in six different directions. The cooling rate dependence of TRM intensity was also analyzed for each specimen by applying a supplementary cycle of measurements consisting of four TRM acquisition steps and performed during the Thellier experiments. During the archaeointensity experiments, the typical laboratory cooling time is about 1.5 hours. Archaeological information, however, indicates that the natural cooling time corresponding to the manufacture of the ceramics could be much higher and, in some cases, can last one day. In order to estimate the cooling rate effect upon TRM intensity, we used a slow cooling time of about 12 hours which is considered to approximate the natural cooling time. The comparison between rapid (about 1.5 hours) and slow cooling results (about 12 hours) has been used to quantify the cooling rate effect upon TRM intensity estimates at specimen level. A detailed description of the TRM anisotropy and cooling rate experimental protocols can be found in Gómez-Paccard et al. (2006c).

5. New archaeointensity data from Greece

Archaeointensity determinations were attempted on 125 specimens coming from the four different archaeological sites. The obtained results were plotted and interpreted using NRM-TRM (Arai) diagrams together with the corresponding Zijderveld plots (Fig. 5). Two types of behaviour during Thellier experiments have been observed. Most of the specimens show a very weak secondary component that was easily removed at the first, low temperature steps. After the removal of this soft component, they showed a well-defined straight line going toward the origin of the Zijderveld diagrams (Fig. 5a-d). This component is very stable and most probably corresponds to the TRM acquired during the manufacture of the pottery fragments. The maximum unblocking temperatures observed range between 470 ºC (e.g., Fig. 5a) and 590 ºC (e.g., Fig. 5d), which is in agreement with the rock magnetic results. For

these specimens linear plots in the Arai diagram have been observed (Fig. 5 a-d). Nevertheless, there is a second group of samples that show a more complex or unstable behaviour during the experiments (two clear components of magnetization in the Zijdelverd diagrams, concave NRM-TRM plots and/or clear magneto-chemical alteration during heating). These specimens have not been considered for further analysis (Fig. 5 e, f).

Several criteria were used to select specimens with acceptable Thellier experiments and they are summarized in Table 2. These criteria are mainly based on the linearity of the NRM-TRM, the quality factors proposed by Coe et al. (1978), the maximum angular deviation (MAD, Kirschvink 1980) and the deviation angle DANG (Selkin & Tauxe, 2000). Following Chauvin *et al*. (2005) the maximum potential error of the paleointensity caused by acquisition of chemical remanent magnetization (CRM parameter give as a percentage of the applied field) must be lower than 15%. However, it should be noted that the DANG or the CRM parameter are not always sufficient criteria to detect mineralogical changes if the direction of the NRM and the magnetic laboratory field are sub parallel during Thellier experiments (Hervé *et al*. 2011). A total of 54 archeointensity results satisfied the applied selection criteria and were considered reliable (Table 3). Additionally, 7 specimens with MAD values between 5 and 10º and 1 specimen with a DANG value ~8º were also retained as they satisfied all the other criteria.

During the preparation of the salt- pellets, no control about the position of the specimens inside them was possible and thus no inferences of the direction of the principal axes of the TRM anisotropy tensor can be achieved. Only differences between the uncorrected and TRM anisotropy corrected archaeointensities can be analyzed (Fig. 6a). In general such differences (expressed as a percentage of the TRM anisotropy corrected values) are lower than 20% although for some specimens can reach higher values, up to ~30%. The important effect of TRM anisotropy upon TRM intensity is consistent with the kind of material analysed (e.g., Chauvin et al., 2000). Cooling rate corrections led to differences between uncorrected and cooling rate corrected intensities lower than 10% for all the specimens except four. The highest value is ~35% for specimen TP-7. This value is quite high compared to the value obtained for the sister specimen (TP-7a) or other values from the same collection (Table 3) and although no indication of magnetic alteration is present was considered as unreliable. These results confirm the need to perform TRM anisotropy and cooling

rate corrections when ceramic fragments are studied in order to obtain reliable archaeointensities.

In general, archaeointensity determinations for sister specimens are very similar (e.g., sample PRCA-02 and SKS-04); nevertheless, in some cases, differences are also observed (e.g., sample TP-05). However, no systematic differences have been noticed between the salt pellet and the untreated samples (Table 3). This indicates that the preparation of salt pellet samples can be a reliable solution for the cases where the original ceramic fragments are too small or too thin to allow the preparation of palaeomagnetic samples of standard dimensions. In order to calculate mean fragment intensities at least two specimens per fragment were considered and only mean-fragment intensities for which the standard deviation is lower than 10 % of the intensity value have been considered. The weighting factor w defined by Prévot et al. (1985) was used in order to calculate weighted mean-fragment intensities. This factor takes into account the different qualities of the archaeointensity determinations as expressed by the quality parameters given in Table 3 (Coe et al., 1978; Prévot et al., 1985).

Mean site intensities were calculated using at least two mean fragment intensities. Four new archaeointensity values ranging from 53.6 ± 4.1 to 69.3 ± 3.9 μT have been obtained for Greece. The standard deviations around the means are lower than 10% for ARH and SKS (5.6 % and 7.6% respectively) and higher than 10% for PAROS and TEMPI (11.1 % and 16.8 % respectively). These s.d. values are of the same order than most of the available archaeointensity data (e.g., Genevey et al., 2008; Donadini et al., 2009) and are probably linked to the precision limit of the archeointensity method and/or different ages of the ceramic fragments inside the interval proposed by archaeologists (Gómez-Paccard et al., 2006; Hill et al., 2007).

6. Discussion

6.1 Comparison with previous available archaeointensity data

In order to compare our new results with previous available data, the new intensities have been relocated at the latitude of Thessaloniki (40.60^{o} N) through the virtual axial dipole moment. The compilation of previous data available from Greece and nearby countries (data within a 700 km circle around Thessaloniki) recently published by Tema & Kondopoulou (2011) has been used. However, as thoroughly

discussed by Chauvin et al. (2000) and De Marco et al. (2008), not all the archaeointensity data can be regarded as equally reliable. The establishment of objective criteria to select the most reliable data is certainly a very difficult task. Nevertheless, this is a crucial issue if refined descriptions of geomagnetic field intensity changes are to be obtained. In this study, only the intensity data obtained from at least three specimens, characterized by relative standard deviation lower than 10% and dated within an age uncertainty lower than 300 years have been retained. It is worth to notice that the number of independent samples is often not clear in the available published results (Genevey et al., 2008). For this reason the number of specimens has been used. However, future archaeomagnetic studies must be focused on the study of several independent fragments/ samples per site.

In order to discriminate the reliability of the retained data, a classification and a weighting of the data were performed following the procedure proposed and analytically described by Chauvin et al. (2000). Three weights were defined, one for the technique used, one for the number of samples per site and one for the type of materials studied. Due to often missing information as already pointed above, the number of specimens has been used here instead of the number of samples, although the best approach would have been to consider the number of independent samples. The maximum total weight is 16 and corresponds to these studies where the classical Thellier archaeointensity method has been used accompanied by TRM anisotropy and cooling rate corrections, more than 5 specimens/ samples have been analysed and material usually characterized by small anisotropy of TRM (kilns rather than ceramics) have been studied (Chauvin et al., 2000; De Marco et al., 2008). For our dataset, we obtained weights between 9 (considered less reliable) and 16 (more reliable). It is worth to notice that only 5 archaeointensities coming from the most recent studies correspond to the maximum weight (De Marco et al., 2008; Hill et al., 2008; Tema et al., 2010). Another set of 60 previous data, together with the new intensities for Greece presented here, are also considered as highly reliable with weight equal to 14 or 15 (Fig. 7a). All the weighted archaeointensities are plotted versus their age in Fig. 7a together with the new results.

Comparison with previously existing results shows a good agreement between the new data and those from the literature (Fig. 7a). The intensity obtained for the SKS site is in good agreement with other data from the Early Bronze age even though the number of data available for the 2300-2000 BC period is very limited. Excellent

agreement can be observed between the ARH result and the archaeointensity from a kiln in Bulgaria (Kovacheva et al., 2009) that reduced at Thessaloniki is 67.6± 1.7 μT. However, more high quality data are still needed in order to confirm intensity values of around 70 μT for this period. The archaeointensity determined from the ceramic collection of Paros (PAR) is close to other intensity results available from the same period. However, comparison between the PAR site mean intensity (68.7 ± 7.6 μT, relocated at Thessaloniki) and the intensity obtained from the study of a contemporaneous kiln (PAR1) from the same archaeological site (De Marco et al., 2008), which gives a value of 60.1 ± 5.2 μT (relocated at Thessaloniki), shows a difference of about 9 μT. Differences of about 5-10 μT between contemporaneous sites are of the same order than those observed in other regional datasets (Genevey et al., 2008), even if only high quality data are considered (Gómez-Paccard et al., 2006c; 2008). TEM intensity is in satisfactory agreement with other results from the same time period but it fits better the lower intensities.

6.2 Comparison with regional SV curves and geomagnetic field models

The new Greek intensity results have also been compared with the Greek (De Marco et al., 2008) and the Balkan (Tema & Kondopooulou, 2011) intensity reference SV curves (Fig. 7b) as well as with the predictions of global (Valet et al., 2008; Korte & Constable, 2005; Korte et al., 2009) and regional (Pavón-Carrasco et al., 2009; 2010) geomagnetic field models (Fig. 7c).

The Greek intensity SV curve is based on 336 data from Greece, western Turkey and Former Yugoslavia and has been calculated using the Bayesian statistics (De Marco et al., 2008). The Balkan SV curve is established applying the moving window technique on a reference dataset of 625 intensity results included within a 700 km circle around Thessaloniki, mainly coming from Greece, Bulgaria, Serbia and South Italy (Tema & Kondopoulou, 2011). Comparison of the new data with the Greek and Balkan SV curves (Fig. 7b) shows a good agreement for almost all sites, when the error bars of both data and curves are considered. The intensity calculated for SKS fits well the Balkan curve and it is included in the 95% confidence envelope of the Greek curve. The ARH intensity fits both the Balkan and Greek SV curves at their upper error band limit and seems to support the high intensity shown for this period mainly if its younger 1516 BC age limit is favoured. The intensity calculated from the PAR ceramic fragments, even though it is in good agreement with other data

from the same time period (Fig. 7a) and included in the uncertainty band of the Balkan SV curve, it is around 8 μT higher than the Greek SV curve for the 100 BC to 100 AD period. A possible reason for such difference could be some inaccuracies on the reference data of the Greek curve that for this period includes a large number of low intensities characterised by low reliability according to the weight assigned by De Marco et al. 2008 (Fig. 11 in De Marco et al. 2008). The TEM result is in very good agreement with both the Greek and Balkan SV curves.

During the last years, apart from the local SV curves, several global geomagnetic field models have been proposed to describe the geomagnetic field variations in the past. Korte & Constable (2005) produced a continuous global geomagnetic field model, CALS7K.2 that is determined by regularized least squares inversion of archaeomagnetic, volcanic and lake sediment data using spherical harmonics in space and cubic B splines in time for the past 7000 years. More recently, Korte et al. (2009) proposed the ARCH3K.1 archaeomagnetic model using only data from archaeological material and volcanic rocks covering the last 3 millennia. An intermediate approach between global models and local SV curves is the calculation of regional models. Pavón-Carrasco et al. (2009) has used only archaeomagnetic determinations from archaeological material and calculated a regional archaeomagnetic model (SHA.DIF.3K) that produces the geomagnetic field variations in Europe for the last 3000 years, modelling together the three geomagnetic field elements. Pavón-Carrasco et al. (2010) have recently extended the SCHA.DIF.3K model back in time, up to 6000 BC, and proposed the SCHA.DIF.8K regional model that is based on a selected compilation of both sedimentary and archaeomagnetic data (Pavón-Carrasco et al., 2010). Comparison of the new data with the models' results (Fig. 7c) shows a very good agreement for the SKS and TEM results and some differences for the ARH and PAR determinations. The SKS intensity fits well the SCHA.DIF.8K curve and confirms that for the BC periods the CALS7K.2 model shows lower intensities than those determined by the archaeomagnetic data as already noticed in previous studies (Valet et al., 2008; De Marco et al., 2008; Tema & Kondopoulou, 2011) and therefore it should be cautiously used for archaeomagnetic purposes. The TEM result fits greatly the SCHA.DIF.3K curve and it is in good agreement with the ARCH3K.1 and CALS7K.2 models for the 500 AD period. The PAR intensity is higher than the models results for the 100BC-100 AD but fits them if its lower intensity limit is considered. On the contrary, the ARH intensity does not fit

neither the CALS7K.2 nor the ARCH3K.1 curve. The most probable reason for this difference is that for this period, the regional and global model predictions show very smooth intensity variations, probably due to the use of lake sediment data in the reference datasets which tend to smooth the variation pattern (Pavón-Carrasco et al., 2010). Indeed for the BC periods the models show an importantly smoother variation path when compared with the reference archaeointensity data (Fig. 7a) and the local SV curves (Fig. 7b). This confirms that new reliable archaeointensity data are still needed in order to better refine the geomagnetic field models.

6.3 Geomagnetic intensity changes in Greece for the last five millennia

The new data obtained together with previously published ones confirm that important changes of the Earth's magnetic field occurred in Greece during the last five millennia. Low intensities around 40μT are well constrained for 2700 BC and a clear intensity increase of around 15 μT is noticed up to 2500 BC. The limited number of data for the 2300-700 BC period do not permit a detailed description of the intensity variations for this period but a constant increase of the field intensity can still be recognised. Two high reliability results show high intensities around 700 and 300 BC. Undoubtedly more high quality results are necessary to confirm a possible intensity maximum at 700 BC. For the 300-200 BC it is interesting to notice that there is an important dispersion of data even when only the most reliable data with weights higher than 14 are considered (Fig. 7a). Such dispersion could be explained by errors on the dating of the sites. However, it also shows that even when high quality procedures for archaeointensity determinations are followed, with continuous control of mineralogical changes through pTRM checks, TRM anisotropy and cooling rate corrections, the study of several specimens per sample and the application of strict selection criteria to the results, there is still a dispersion between sites of the same age. This dispersion could be also related to the archaeointensity experimental protocols and to the kind of material analysed. For the Roman period only small intensity variations are noticed in Greece. An abrupt intensity increase can be seen around 700 AD. A second intensity maximum around 900 AD is well demonstrated by at least four high quality results available for the 800-1000 AD period. On the contrary, the intensity peak seen around 1600-1700 AD is defined by only lower weight data and more high quality data for this period are needed to confirm it. From 1700 AD to nowadays the geomagnetic field's intensity is constantly decreasing.

Many of the main characteristics of the geomagnetic field variations in Greece are well described by the SV curves for Greece and Balkans and the regional and global geomagnetic field model results but there are still some features that can not be clearly seen in these reference curves. Both the Greek and the Balkan curves successfully describe the intensity variation for the 3000-2500 BC, the high intensity peak around 400-500 BC and the small variations during the Roman period. The Balkan curve also show two intensity peaks around 600 and 900 AD in good agreement with the high quality data. Nevertheless both local SV curves are characterised by large uncertainty envelopes that do not allow the detailed description of the fine characteristics of the geomagnetic field intensity variations at small time scale. On the other hand, the regional and global models, even if they are based on a very large number of data and show detailed variations for the last 3000 years, it seems that still they do not successfully fit the high intensity periods (e.g., 300 BC and 600 AD). For the BC periods, regional and global models show very smooth intensity variations and do not fit most of the reference data. This clearly shows that more attention should be pointed on the reliability of the reference data used for regional and global modelling. The use of sedimentary data should also be avoided if the detailed short term intensity variations are to be described, for which the maximum precision is desired.

7. Conclusions

Four new high quality archaeointensity data have been obtained from four ceramic collections with ages from 2200 BC to 565 AD. Several selection criteria have been applied for the acceptance of only the most reliable intensity determinations. The archaeointensity experiments carried out using the classical Thellier method (with pTRM checks and anisotropy of TRM and cooling rate corrections) give *in situ* mean intensities ranging from 53.6 ± 4.1 to 69.3 ± 3.9 μT with corresponding VADM values from 9.2 ± 0.7 to 11.9 ± 0.7 x 10^{22} Am^2. The new results are reasonably consistent with previous data, with the SV reference curves for Greece and the South Balkan Peninsula and with regional and global geomagnetic field models results. The new data obtained combined with previously published data confirm that important changes of the Earth's magnetic field occurred in Greece during the last five millennia. This illustrates the potential of geomagnetic field intensity changes as a dating tool in this area. However, for some periods, the

available archaeointensity data for the Balkan area show a large dispersion, even for data reaching high quality standards. This dispersion could be explained by age uncertainties but also by the precision limit of the experimental protocols followed to determine past archaeointensities. To better constrain the evolution of the Earth's magnetic field strength in Greece for the last five millennia, it is therefore necessary to have as many as possible well and precisely dated (if possible with age errors less than a century) and high-quality archaeointensity determinations from several independent studies per time period, as it is already done for constructing SV directional curves.

Acknowledgments

Miriam Gómez-Paccard acknowledges the financial support given by a CSIC JAE-Doc postdoctoral research contract (MGP), the Spanish Ministry of Education and Science (project: CGL2008-02203/BTE) and Banco Santander - Universidad Complutense de Madrid (Grupo de Investigación 910396). Despina Kondopoulou has benefitted from the hospitality and laboratory use of the Section de Physique du Globe, Insitut Royal Meteorologique de Belgique, and Drs. J.Hus and S.Spassov are warmly thanked. The archaeologists Dr. Ch. Koukouli-Chrysanthaki, Dr. E. Hasaki, Mrs. S. Sdrolia and Mr. G. Deliopoulos are highly acknowledged for sampling permission and archaeological information provided.

References

Chauvin, A., Garcia, Y., Lanos, Ph., Laubenheimer, F., 2000. Paleointensity of the geomagnetic field recovered on archaeomagnetic sites from France. *Phys. Earth Planet. Int*., 120, 111-136.

Chauvin, A., Roperch, P., Levi, S., 2005. Reliability of geomagnetic palaeointensity data: the effects of the NRM fraction and concave-up behaviour on palaeointensity determinations by the Thellier method. *Phys. Earth Planet. Int..*, 150, 265–286. doi:10.1016/j.pepi.2004.11.008.

Coe, R. S., Grommé, S., Mankinen, E. A., 1978. Geomagnetic paleointensities from radiocarbon-dated lava flows on Hawaii and the question of the Pacific non dipole low. *J. Geophys. Res.*, 83 (B4), 1740-1756.

De Marco, E., 2007. Integrated magnetic and archaeomagnetic measurements in archaeological sites: contribution to secular variation curves for Greece. Ph.D. thesis, Aristotle University of Thessaloniki, Thessaloniki, Greece, pp. 293.

De Marco, E., Spatharas, V., Gómez-Paccard, M., Chauvin, A., Kondopoulou, D., 2008. New archaeointensity results from archaeological sites and variation of the geomagnetic field intensity for the last 7 millennia in Greece. *Phys. Chem. Earth*, 33, 578-595.

Deliopoulos, G., 2007. The ceramics of the «stone basement» phase in the prehistoric settlement of Archontiko-Giannitsa. Master Thesis, Aristotle University of Thessaloniki, Thessaloniki, Greece, pp. 154 *(in Greek).*

Donadini, F., Korte, M., Constable, C. G., 2009. Geomagnetic field for 0–3 ka: 1. New data sets for global modelling. *Geochem. Geophys. Geosyst.*, 10, Q06007, doi:10.1029/2008GC002295.

Downey, W.S. & Tarling, D.H., 1984. Archaeomagnetic dating of Santorini volcanic eruptions and fired destruction levels of Late Minoan civilization. *Nature*, 309, 519-523.

Evans, M.E., 1986. Palaeointensity estimates from Italian kilns. *J. Geomag. Geoelectr.*, 38, 1259–1267.

Gallet, Y., Genevey, A., Le Goff, M., 2002. Three millennia of directional variation of the Earth's magnetic field in Western Europe as revealed by archaeological artefacts. *Phys. Earth Planet. Inter*., 131, 81-89.

Genevey, A., Gallet, Y., Constable, C., Korte, M., Hulot, G., 2008. ArcheoInt: An upgraded compilation of geomagnetic field intensity data for the past ten millennia

and its application to recovery of the past dipole moment. *Geochem. Geophys. Geosyst*., 9, Q04038, doi: 10.1029/2007GC001881.

Gómez-Paccard, M., Catanzariti, G., Ruiz-Martinez, V.C., McIntosh, G., Núñez, J.I., Osete, M.L, Chauvin, A., Lanos, Ph., Tarling, D.H., Bernal-Casasola, D., Thiriot, J., and "Archaeological Working Group", 2006a. A catalogue of Spanish archaeomagnetic data. Geophys. J. Int., 166, 1125–1143, doi:10.1111/j.1365-246X.2006.03020.x.

Gómez-Paccard, M., P. Lanos, A. Chauvin, G. McInstosh, M. L. Osete, G. Catanzariti, V. C. Ruiz-Martınez, Núnez, J. I., 2006b. First archaeomagnetic secular variation curve for the Iberian Peninsula: Comparison with other data from Western Europe and with global geomagnetic field models. *Geochem. Geophys. Geosyst.,* 7, Q12001, doi:10.1029/2006GC001476.

Gómez-Paccard, M., Chauvin, A., Lanos, P., Thiriot, J., Jiménez-Castillo, P., 2006c. Archaeomagnetic study of seven contemporaneous kilns from Murcia (Spain). *Phys. Earth Planet. Int.,* 157, 16-32.

Gómez-Paccard, M., Chauvin, A., Lanos, P., Thiriot, J., 2008. New archaeointensity data from Spain and the geomagnetic dipole moment in Western Europe over the past 2000 years. *J. Geophys. Res.*, 113 (B9), B09103.

Hervé, G., Schnepp, E., Chauvin, A., Lanos, P., Nowaczyk, N., 2011. Archaeomagnetic results on three Early Iron Age salt-kilns from Moyenvic (France). *Geophys. J. Int.*, 185, 144-156, doi: 10.1111/j.1365-246X.2011.04933.x

Hill, M., Lanos, Ph., Chauvin, A., Vitali, D., Laubenheimer, F., 2007. An archaeomagnetic investigation of a Roman amphorae workshop in Albinia (Italy). *Geophys. J. Int.*, 169, 471-482.

Kirschvink, J.L., 1980. The least-squares line and plane and the analysis of paleomagnetic data. *Geophy. J. Royal Astr. Soc.*, 62, 699-718.

Korte, M. & Constable, C.G., 2005. Continuous geomagnetic field models for the past 7 millennia: 2.CALS7K. *Geochem. Geophys. Geosyst.*, 6, Q02H16, doi: 10.1029/2004GC000801.

Korte, M., Donadini, F., Constable, C. G., 2009. Geomagnetic field for 0–3 ka: 2. A new series of time-varying global models. *Geochem. Geophys. Geosyst*., 10, Q06008, doi:10.1029/2008GC002297.

Korte, M., Genevey, A., Constable, C., Frank, U., Schnepp, E., 2005. Continuous geomagnetic field models for the past 7 millennia: 1. A new global data compilation. *Geochem. Geophys. Geosyst.*, 6, Q02H15, doi:10.1029/2004GC000800.

Koukouli-Chrysanthaki, Ch., 1989. An early Bronze age in Skala Sotiros, Thasos. In *Archaeological Works in Macedonia and Thrace*, *AEMTH*, 3, 507-512, (*in Greek*).

Koukouli-Chrysanthaki, Ch., 1990. Excavation in Skala Sotiros 1990. In *Archaeological Works in Macedonia and Thrace*, *AEMTH*, 4, 531-545, *(in Greek)*.

Kovacheva, M., Boyadziev, Y., Kostadinova-Avramova, M., Jordanova, N., Donadini, F., 2009. Updated archaeomagnetic data set of the past 8 millennia from the Sofia laboratory, Bulgaria. *Geochem. Geophys. Geosyst.*, 10, Q05002, doi: 10.1029/2008GC002347.

Lowrie, W., 1990. Identification of ferromagnetic minerals in a rock by coercivity and unblocking temperature properties. *Geophys. Res. Lett.*, 17, 159-162.

Maniatis, Y., Facorellis, Y., Pilali, A., Papanthimou-Papaefthimiou, A., 2002. Firing temperature determinations of low fired clay structures. In: *Modern Trends in Scientific Studies on Ancient Ceramics*, BAR International Series, 1011, 59-68.

Papadopoulou, E., 2002. Small clay findings from Archontiko-Giannitsa. Master Thesis, Aristotle University of Thessaloniki, Thessaloniki, Greece (*in Greek*).

Pavón-Carrasco, F. J., Osete, M.L., Torta, J. M., Gaya-Piqué, L. R., 2009. A regional archaeomagnetic model for Europe for the last 3000 years, SCHA.DIF.3K: applications to archaeomagnetic dating. *Geochem. Geophys. Geosyst.*, 10 (3), Q03013, doi:10.1029/2008GC002244.

Pavón-Carrasco, F. J., Osete, M.L., Torta, J., 2010. Regional modeling of the geomagnetic field in Europe from 6000 BC to 1000 BC. *Geochem. Geophys. Geosyst*, 11, Q11008, doi: 10.1029/2010GC003197.

Pick, T. & Tauxe, L., 1993. Holocene palaeointensities: Thellier experiments on submarine basaltic glass from the East Pacific Rise. *J. Geophys. Res.*, 98, 17949-17964.

Prévot, M., Mankinen, E.A., Coe, R.S., Grommé, C.S., 1985. The Steens Mountain (Oregon) Geomagnetic Polarity Transition. 2. Field Intensity Variations and Discussion of Reversal Models. *J Geophys. Res*., 90, 10417-10448.

Rodriguez Ceja, M., Goguitchaichvili, A., Morales, J., Ostrooumov, M., Manzanilla, L. R., Aguilar Reyes, B., Urrutia-Fucugauchi, J., 2009. Integrated archaeomagnetic and micro–Raman spectroscopy study of pre-Columbian ceramics from the Mesoamerican formative village of Cuanalan, Teotihuacan Valley, Mexico. *J. Geophys. Res*., 114, B04103, doi:10.1029/2008JB006106.

Schnepp, E. & Lanos, Ph., 2005. Archaeomagnetic secular variation in Germany during the past 2500 years. *Geophys. J. Int.*, 163, 479-490.

Schnepp, E., Pucher, R., Reindeers, J., Hambach, U., Soffel, H. & Hedley, I., 2004. A German catalogue of archaeomagnetic data. *Geophys. J. Int.*, 157, 64-78.

Sdrolia, S., 2009. Palaeochristian findings in the region of Kissavos. *Proceedings of the third Archaeological Symposium of Thessaly*, Volos, Greece. *In press*

Selkin, P. A. & Tauxe, L., 2000. Long-term variations in palaeointensity. Phil. Trans. R. Soc. Lond. A, 358, 1065-1088.

Spatharas, V., Kondopoulou, D., Aidona, E., Efthimiadis, K., 2011.New magnetic mineralogy and archaeointensity results from Greek kilns and baked clays. *Stud. Geophys. Geod.*, 55, 131-157

Tema E., Hedley, I., Lanos, Ph., 2006. Archaeomagnetism in Italy: a compilation of data including new results and a preliminary Italian secular variation curve. *Geophys. J. Int.*, 167, 1160-1171. doi:10.1111/j.1365-246X.2006.03150.x

Tema, E. & Kondopoulou, D., 2011. Secular variation of the Earth's magnetic field in the Balkan region during the last 8 millennia based on archaeomagnetic data. *Geophys. J. Int.*, in press

Thellier, E. & Thellier, O., 1959. Sur l'intensité du champ magnétique terrestre dans le passé historique et géologique. *Ann. Geophys.*, 15, 285-376.

Valet, J.P., Herrero-Bervera, E., LeMouël, J.L & Plenier, G., 2008. Secular variation of the geomagnetic dipole during the past 2000 years. *Geochem. Geophys. Geosyst.*, 9, Q01008, doi: 10.1029/2007GC001728.

Table caption

Table 1. Information about the location and archaeological ages of the the studied ceramics.

Table 2. Reliability of archaeointensity determinations: selection criteria used in this study for retaining only high-quality intensity determinations.

Table 3. Summary of the new archaeointensity results. Site, (Age), name of the archaeological site where the material has been recovered, (archaeological age of the site); Name, name of the specimen studied (same numbers indicate specimens corresponding to the same fragment); Lab., name of the laboratory where the archaeointensity experiments were performed; Type of sample, description of the type of sample analyzed; T_{min} −T_{max}, temperature interval used for the slope calculation in ^{o}C; n, number of data points within this temperature interval; f, fraction of the NRM component used in the slope calculation; g, gap factor; q, quality factor; MAD, maximum angle of deviation; DANG, deviation angle; CRM, potential error on the estimation of the paleointensity due to the acquisition of CRM as a percentage of the applied field; β, ratio of the standard error of the slope to the absolute value of the best-fit slope for the data on the NRM-TRM diagram; F ± σF, mean intensity and standard deviation per sample without TRM anisotropy correction; Fe, mean intensity per sample with correction of TRM anisotropy; Fm ± s.d., TRM anisotropy corrected mean intensity per fragment and standard deviation; Fpo, weighted mean intensity per fragment; ΔTRM (12 h), correction factor per sample for a cooling time of about 12 h; alt (12 h), alteration factor per sample for a cooling time of about 12 h; Fpocr, weighted mean intensity per sample after TRM anisotropy and cooling rate corrections. Site mean: n= number of specimens used for the calculation of the final mean intensity; N= number of samples; F ± sd= final mean intensity per site after TRM anisotropy and cooling rate corrections and standard deviation; F_{Thes} ± sd= final mean intensity per site and standard deviation calculated at the latitude of Thessaloniki (40.60 ^{o}N); VADM= virtual axial dipole moment calculated using the mean intensities corrected both for the cooling rate and TRM anisotropy effects.

Figure captions

Fig. 1. Location of the studied sites.

Fig. 2. Representative continuous magnetic susceptibility versus temperature curves.

Fig. 3. Representative isothermal remanent acquisition (IRM) curves for the four sites.

Fig. 4. Thermal stepwise demagnetization of three IRM components for representative samples. Symbols: dot = low- (0.1 T); diamond = intermediate- (0.5 T); square = high- (1.3 T) coercivity component.

Fig. 5. Examples of NRM-TRM diagrams and associated Zijderveld and NRM decay diagrams from a-d) successful and e-f) rejected archaeointensity experiments. F is the archeointensity determined, f, the fraction of the NRM used for slope computation and q the quality factor. Black (white) dots in the NRM-TRM diagrams indicate the points considered (rejected) for slope computations.

Fig. 6. Effect of the a) TRM anisotropy and b) cooling rate effect upon TRM acquisition. Both are expressed as a percentage of the corrected archeointensity values.

Fig. 7. a) The new intensity results (black triangles) plotted versus age together with literature intensity data from the Balkan area (grey and black circles); b) the new data plotted together with the regional SV curves available for Greece and the South Balkan Peninsula; c) CALS7K.2 and ARCH3K.1 global and SCHA.DIF.3K and SCHA.DIF.8K regional geomagnetic field models results. All data are reduced at the latitude of Thessaloniki (40.60^{o} N).

Archaeological Site	Code	Geographic Coordinates	Number of independent fragments	Archaeological Age
Skala Sotiros	SKS	40.73 ^{o} N, 24.55^{o} E	6	2200-2100 BC
Archontico	ARH	40.79^{o} N, 22.47 ^{o} E	9	1516-1414 BC
Paros	PAR	37.08 ^{o} N, 25.15^{o} E	10	100 BC-100AD
Tempi	TEM	39.86 ^{o} N, 22.53^{o} E	9	518-565 AD

Table 1

1

Reliability of archeointensity determinations : selection criteria used for retaining archeointensity results	
At specimen level	Well defined straight lines going through the origin in the Zijderveld diagrams MAD (Kirschvink 1980) and DANG (Selkin & Tauxe 2000) must be lower than 5º. The archeointensity is determined using the same temperature interval for which the primary magnetic component was isolated Linear segments in the NRM-TRM plots At least 5 temperature steps and ~50% of the initial NRM must be involved for slope computation Maximum potential error caused by chemical remanent magnetization (CRM parameter) must be lower than 15% (normalized by the applied field) The ratio of the standard error of the slope to the absolute value of the best-fit slope for the data on the NRM-TRM diagram (β parameter) must be lower than 0.05 Positive pTRM checks: maximum difference between the original pTRM and the pTRM check of about 10% of evolution normalised by the total TRM The effect of TRM anisotropy upon TRM acquisition must be considered The effect of cooling rate correction upon TRM acquisition must be investigated. Magnetic alteration during the cooling rate procedure must be lower than the cooling rate factor applied to archeointensity estimations.
At fragment level	At least two specimens per fragment must be considered in order to calculate mean intensities per fragment We fixed a limit of ~10% for the standard deviation around mean intensities per fragment (normalised by mean intensity values)
At age group level	At least two fragments per site in order to calculate site mean intensities

2
3
4 Table 2
5

Site	Name	Lab	Type of sample	T_{min}-T_{max}	n	f	g	q	MAD	DANG	CRM	β	F ± σF	F_e	Fm ± sd	Fpo	ΔM (12h)	alt. (12h)	Fpocr
Age (years)				(°C)					(°)	(°)	(%)		(μT)	(μT)	(μT)	(μT)	(%)	(%)	(μT)
TEMPI	TEM-1A	Barcelona	salt pellet	150-500	9	0.74	0.86	46.8	7.0	1.3	11.2	0.01	48.0 ± 0.66	51.1	49,8 ± 2,3	48.9	1.9	-3.2	48.1
(518-565 AD)	TEM-1B	Barcelona	salt pellet	150-530	10	0.79	0.88	100.9	3.8	1.1	3.5	0.01	45.4 ± 0.31	47.2			3.0	-2.1	
	TEM-1C	Torino	salt pellet	100-440	8	0.69	0.85	22.5	2.8	1.9	3.4	0.03	63.9 ± 1.67	51.2			-0.5	-0.4	
	TEM-2A	Barcelona	salt pellet	200-500	8	0.64	0.83	16.7	3.8	2.6	5.7	0.03	58.9 ± 1.87	45.7	49,1 ± 4,6	50.9	3.4	1.1	49.7
	TEM-2B	Barcelona	salt pellet	200-530	9	0.72	0.87	32.7	2.5	0.6	2.3	0.02	60.4 ± 1.15	47.4			3.7	0.1	
	TEM-2C	Torino	salt pellet	150-470	8	0.69	0.84	56.6	2.1	1.0	3.5	0.01	55.4 ± 0.57	54.3			0.9	1.0	
	TEM-4A	Barcelona	salt pellet	150-440	7	0.57	0.78	13.6	4.4	0.4	5.9	0.03	45.6 ± 1.5	48.2	51,3 ± 3,3	50.9	1.3	0.7	50.4
	TEM-4B	Barcelona	salt pellet	150-440	7	0.57	0.79	9.4	3.3	1.6	4.3	0.05	52.0 ± 2.5	54.7			2.3	-0.7	
	TEM-4C	Torino	salt pellet	150-470	8	0.75	0.83	30.3	2.0	0.5	2.8	0.02	56.3 ± 1.15	51.0			0.3	-0.4	
	TEM-5A	Barcelona	untreated cube	100-400	7	0.73	0.75	29.9	2.6	2.4	6.4	0.02	78.1 ± 1.44	72.2	74,0 ± 3,4	73.7	0.2	-4.7	73.7
	TEM-5C	Torino	salt pellet	100-350	6	0.74	0.73	14.5	2.9	1.5	6.6	0.04	81.6 ± 3.01	78.9			0.3	-0.9	
	TEM-5	Torino	untreated cube	200-470	7	0.73	0.70	15.8	4.6	2.4	12.0	0.03	81.0 ± 2.60	73.6			-0.6	-2.0	
	TEM-5B	Barcelona	untreated cube	100-350	6	0.68	0.71	15.6	1.6	0.9	8.4	0.03	70.6 ± 2.17	71.4			0.1	-2.0	
	TEM-6B	Barcelona	untreated cube	100-530	11	0.77	0.86	39.2	3.8	0.8	6.0	0.02	76.7 ± 1.30	65.0	64,0 ± 1,3	64.1	1.9	-3.9	64.8
	TEM-6	Torino	untreated cube	150-530	10	0.69	0.85	35.4	5.4	2.9	7.1	0.02	58.5 ± 0.98	62.5			-13.0	-0.4	
	TEM-6D	Torino	salt pellet	200-470	7	0.71	0.82	35.5	1.0	0.7	1.0	0.02	62.1 ± 1.01	64.5			7.0	-0.1	
	TEM-7	Torino	untreated cube	200-470	7	0.56	0.83	21.9	4.2	1.6	7.0	0.02	62.1 ± 1.31	52.6	53,5 ± 1,3	53.3	35.6	-1.8	53.3
	TEM-7A	Barcelona	salt pellet	200-530	9	0.61	0.85	17.0	4.8	1.8	1.8	0.03	60.3 ± 1.84	54.4			-1.6	-1.2	
	TEM-8A	Barcelona	salt pellet	200-500	8	0.54	0.83	12.2	4.9	3.7	5.7	0.04	46.5 ± 1.71	49.04	51,3 ± 2,9	51.2	2.9	-1.7	49
	TEM-8C	Torino	salt pellet	150-500	9	0.64	0.85	14.2	2.9	4.6	11.0	0.04	56.2 ± 2.16	54.5			5.2	-1.0	

	TEM-8D	Torino	salt pellet	200-530	9	0.67	0.80	20.5	2.4	1.5	3.0	0.03	52.2 ± 1.37	50.4			4.8	-0.3	
	TEM-9B	Barcelona	salt pellet	150-500	9	0.70	0.86	31.2	3.0	0.5	2.6	0.02	51.7 ± 1.00	60.8	63,7 ± 2,7	64.2	1.3	0.2	62.9
	TEM-9C	Torino	salt pellet	150-500	9	0.60	0.86	35.4	2.3	1.4	2.7	0.02	51.5 ± 0.75	64.3			-5.4	1.6	
	TEM-9D	Torino	salt pellet	100-470	9	0.83	0.86	57.7	2.4	1.6	4.8	0.01	53.1 ± 0.66	66.0			6.9	-0.3	
Site mean:	**n= 24**	**N= 8**	**F ± sd = 56.5 ± 9.5 µT**		**F_{Thes} ± sd = 57.0 ± 9.6 µT**			**VADM= 9.78 ± 1.6 (10^{22} Am^2)**											
PAROS	PRCA-02A	Barcelona	untreated cube	150-500	9	0.74	0.82	24.6	2.1	3.9	9.1	0.03	67.8 ± 1.66	69.0	69,1± 0,6	69.1	-2.0	-0.9	67.6
(100 BC-100 AD)	PRCA-02B	Torino	salt pellet	100-470	9	0.76	0.87	22.6	2.3	1.5	4.9	0.03	60.7 ± 1.76	68.6			4.5	-3.0	
	PRCA-02D	Barcelona	untreated cube	200-530	9	0.86	0.84	24.5	3.8	4.3	9.9	0.03	68.2 ± 2.01	69.8			3.7	1.6	
	PRCA-03A	Torino	salt pellet	100-440	8	0.70	0.81	26.4	1.8	2.5	4.5	0.02	66.9 ± 1.43	67.0	65,3± 2,5	64.9	2.7	1.2	62.3
	PRCA-03C	Barcelona	untreated cube	100-500	10	0.88	0.83	47.7	2.3	2.7	10.5	0.02	62.2 ± 0.95	63.5			4.8	-1.2	
	PRCA-04A	Torino	salt pellet	100-470	9	0.86	0.85	43.9	2.5	1.3	4.0	0.02	48.3 ± 0.80	61.6	50,2± 1,8	62.7	5.2	-0.1	60.8
	PRCA-04C	Barcelona	untreated cube	200-470	7	0.58	0.80	27.4	2.9	2.4	5.3	0.02	52.1 ± 0.9	64.1			-3.1	-4.3	
	PRCA-05A	Barcelona	untreated cube	200-530	9	0.57	0.86	18.3	4.4	1.6	3.1	0.03	55.6 ± 1.51	56.5	55,4 ± 1,6	55.6	3.9	-0.7	53.3
	PRCA-05C	Barcelona	untreated cube	200-530	9	0.59	0.87	11.7	3.6	1.0	4.4	0.04	53.6 ± 2.34	54.2			4.0	-1.3	
	PRCA-06A	Barcelona	untreated cube	100-440	8	0.52	0.81	7.7	7.9	4.9	11.5	0.06	66,2 ± 3,6	60.4	62,5 ± 3,0	63.8	-15.9	-5.5	65.7
	PRCA-06C	Torino	salt pellet	100-470	9	0.82	0.86	32.9	2.5	1.5	4.9	0.02	59.1 ± 1.25	64.6			0.9	-2.3	
	PRCA-08B	Barcelona	untreated cube	100-530	11	0.80	0.89	56.6	4.2	1.8	10.8	0.01	60.5 ± 0.76	70.0	68,9 ± 1,6	69.2	1.4	2.2	69.2
	PRCA-08C	Torino	salt pellet	100-470	9	0.72	0.87	31.1	1.5	2.7	3.1	0.02	54.7 ± 1.1	67.8			1.7	-3.0	
	PRCB-01A	Barcelona	untreated cube	100-500	10	0.75	0.87	28.9	2.4	0.6	11.0	0.02	70.3 ± 1.58	73.3	77,0 ± 4,1	76.2	-2.2	-0.1	77.7
	PRCB-01B	Barcelona	untreated cube	100-500	10	0.74	0.87	35.6	1.6	0.2	6.9	0.02	73.7 ± 1.33	76.3			-2.5	-0.2	
	PRCB-01C	Torino	salt pellet	100-440	8	0.68	0.85	13.8	2.5	2.2	6.2	0.04	71.7 ± 3.02	81.4			-0.5	-3.2	

	PRCB-02A	Torino	salt pellet	200-470	7	0.53	0.82	29.0	2.1	3.8	4.4	0.02	58.4 ± 0.87	68.8	73,4 ± 4,8	72.7	6.4	-1.0	70.6
	PRCB-02C	Barcelona	untreated cube	200-530	9	0.73	0.87	21.9	4.6	1.0	11.6	0.03	67.3 ± 1.95	78.4			0.0	6.6	
	PRCB-02D	Barcelona	untreated cube	200-470	7	0.54	0.82	12.4	4.7	1.8	6.4	0.04	91.6 ± 3.3	73.1			-0.3	-0.4	
Site mean:	**n= 19**	**N= 8**	**F ± sd = 65.9 ± 7.3 µT**	**F_{Thes} ± sd = 68.7 ± 7.6 µT**		**VADM= 11.78 ± 1.3 (10^{+22} A m^2)**												
ARH	ARH-1F	Torino	salt pellet	250-560	9	0.69	0.86	29.1	5.1	4.1	13.3	0.02	84.1 ± 1.72	85.7			-10.7	-0.9	
(1516-1414 BC)																			
	ARH-3D	Torino	salt pellet	300-590	9	0.73	0.85	27.5	8.1	2.5	13.9	0.02	66.6 ± 1.51	62.1			-7.9	-1.9	
	ARH-4A	Barcelona	untreated cube	200-560	10	0.68	0.81	11.7	6.5	2.0	11.5	0.05	81.4 ± 3.82	72.9	69,6 ± 4,7	68.3	-8.2	-3.7	69.9
	ARH-4B	Barcelona	untreated cube	200-560	10	0.70	0.84	26.6	4.4	3.5	9.6	0.02	83.5 ± 1.85	66.3			0.5	-1.6	
	ARH-5A	Barcelona	untreated cube	200-590	11	0.88	0.81	29.0	2.2	2.2	3.6	0.03	64.5 ± 1.6	69.0	68,9 ± 0,2	68.9	0.9	-4.6	72.9
	ARH-5B	Barcelona	untreated cube	200-590	11	0.86	0.81	28.4	3.9	3.4	9.1	0.03	61.3 ± 1.5	68.6			-8.8	4.6	
	ARH-5C	Barcelona	untreated cube	200-590	11	0.88	0.80	34.0	2.7	0.9	9.8	0.02	68.6 ± 1.42	69.0			-8.3	-8.0	
	ARH-6D	Torino	salt pellet	200-440	6	0.59	0.75	41.1	3.6	1.6	10.0	0.01	65.7 ± 0.7	69.6			0.2	-0.1	
	ARH-7A	Barcelona	untreated cube	300-530	7	0.62	0.73	14.6	4.4	2.9	8.6	0.03	79.4 ± 2.43	70.2	67,6 ± 3,9	67	2.3	0.3	65.2
	ARH-7B	Barcelona	untreated cube	350-530	6	0.59	0.63	10.0	5.2	1.4	5.1	0.04	66.3 ± 2.44	69.4			7.5	-2.8	
	ARH-7D	Torino	salt pellet	300-500	6	0.59	0.77	16.4	4.5	2.1	6.1	0.03	64.4 ± 1.79	63.1			0.3	-2.7	
Site mean:	**n= 8**	**N= 3**	**F ± sd = 69.3 ± 3.9 µT**	**F_{Thes} ± sd = 69.2 ± 3.9 µT**		**VADM= 11.86 ± 0.67 (10^{+22} A m^2)**												
SKS	SKS-3A	Barcelona	untreated cube	350-560	7	0.73	0.83	30.0	5.3	4.7	10.1	0.02	62.8 ± 1.26	53.3	56,1 ± 5,4	58.6	6.1	-0.5	56.5
(2200-2100 BC)	SKS-3B	Barcelona	untreated cube	350-560	7	0.75	0.82	34.0	5.2	5.3	10.0	0.02	61.1 ± 1.11	53.9			3.4	-1.8	
	SKS-3C	Barcelona	untreated cube	400-590	7	0.63	0.81	30.3	4.4	3.3	6.5	0.02	59.4 ± 1.01	53.1			5.6	-1.0	
	SKS-3D	Torino	salt pellet	300-470	5	0.53	0.74	67.9	1.3	1.9	3.2	0.01	69.8 ± 0.5	64.2			2.5	-3.2	

	SKS-4A	Barcelona	untreated cube	150-530	10	0.71	0.88	33.6	3.2	8.0	11.7	0.02	75.2 ± 1.39	65.7	71,2 ± 6,2	72.4	1.1	-1.7	50.7
	SKS-4B	Barcelona	untreated cube	150-530	10	0.75	0.88	47.0	3.4	5.3	11.4	0.01	75.8 ± 1.07	69.9			0.9	-2.8	
	SKS-4C	Barcelona	untreated cube	150-530	10	0.81	0.88	63.0	3.6	5.2	10.5	0.01	75.3 ± 0.85	77.9			2.7	-5.4	
Site mean:	**n= 7**	**N= 2**	**F ± sd = 53.6 ± 4.1 µT**	**F_{Thes} ± sd = 53.5 ± 4.1 µT**		**VADM= 9.18 ± 0.7 (10^{+22} A m^2)**												

Table 3


E 20°30'
E 22°30'
E 24 °30'
E 26 °30'
F.Y.R.O.M.
BULGARIA
TURKEY
ARH
THESSALONIKI
SKS
N 40 °30'
ALBANIA
N 40 °30'
TEM
TURKEY
N 38 °30'
N 38 °30'
ATHENS
PAR
N 36 °30'
N 36 °30'
E 20°30'
E 22°30'
E 24 °30'
E 26 °30'

Fig. 1

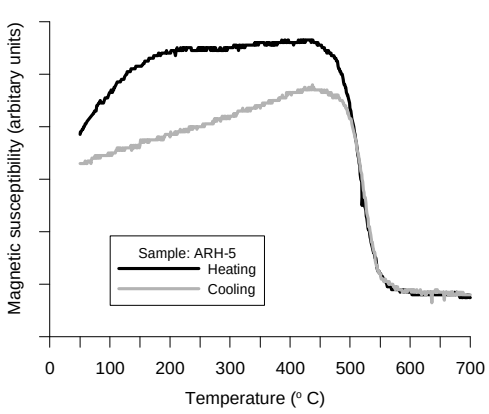
Magnetic susceptibility (arbitary units)
Sample: ARH-5
Heating
Cooling
0
100
200
300
400
500
600
700
Temperature (° C)

(a)

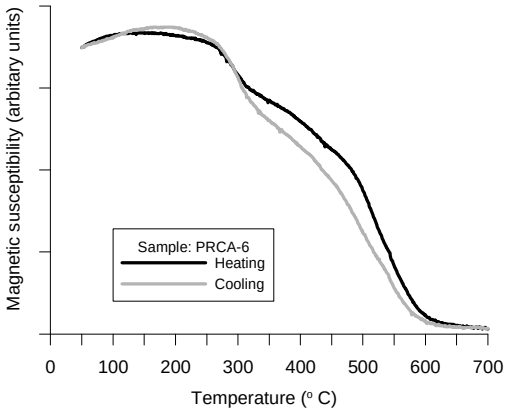
Magnetic susceptibility (arbitary units)
Sample: PRCA-6
Heating
Cooling
0
100
200
300
400
500
600
700
Temperature (° C)

(b)

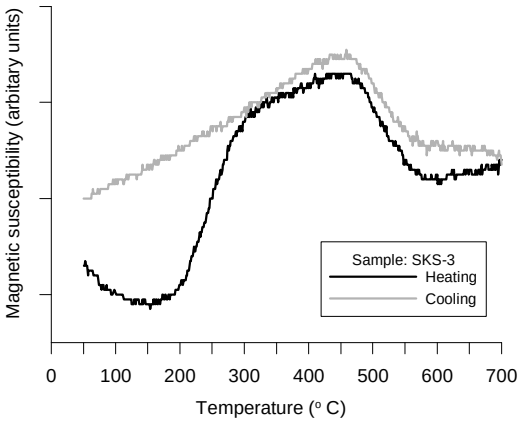
Magnetic susceptibility (arbitary units)
Sample: SKS-3
Heating
Cooling
0
100
200
300
400
500
600
700
Temperature (° C)

(c)

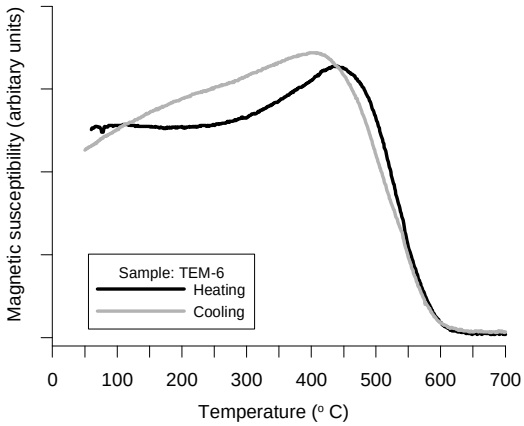
Magnetic susceptibility (arbitary units)
Sample: TEM-6
Heating
Cooling
0
100
200
300
400
500
600
700
Temperature (° C)

(d)

Fig. 2

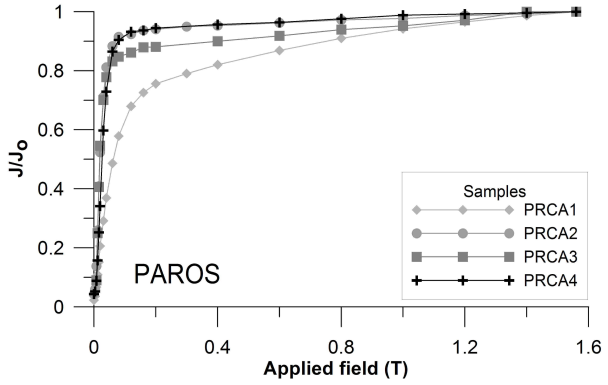
J/Jo
Applied field (T)
PAROS
Samples
PRCA1
PRCA2
PRCA3
PRCA4

a)

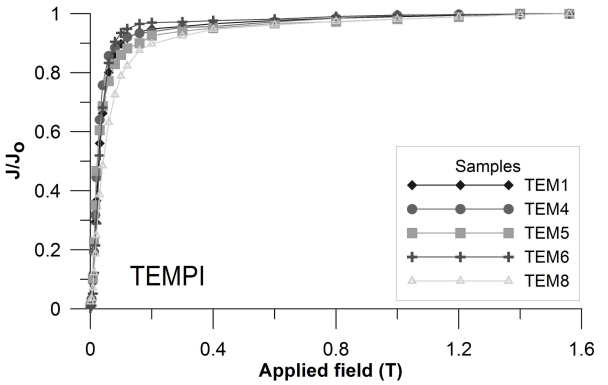
J/Jo
Applied field (T)
TEMPI
Samples
TEM1
TEM4
TEM5
TEM6
TEM8

b)

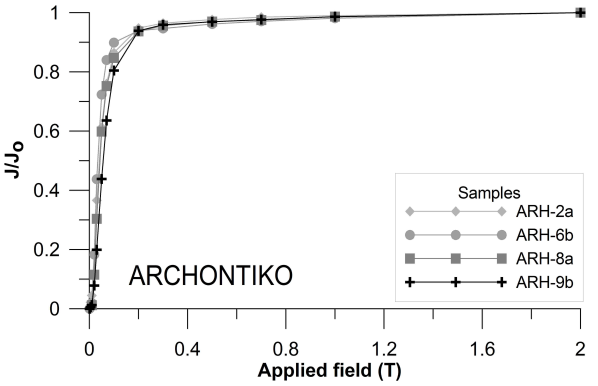
J/Jo
Applied field (T)
ARCHONTIKO
Samples
ARH-2a
ARH-6b
ARH-8a
ARH-9b

c)

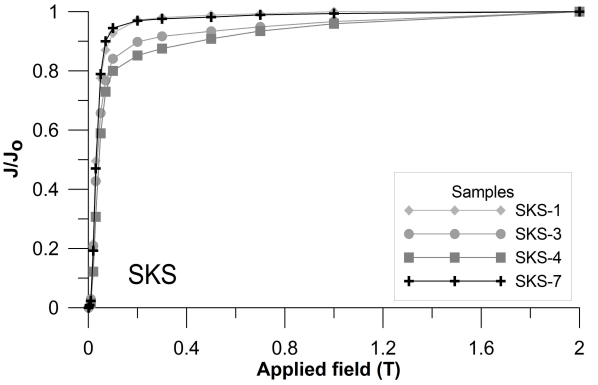
J/Jo
Applied field (T)
SKS
Samples
SKS-1
SKS-3
SKS-4
SKS-7

d)

Fig. 3

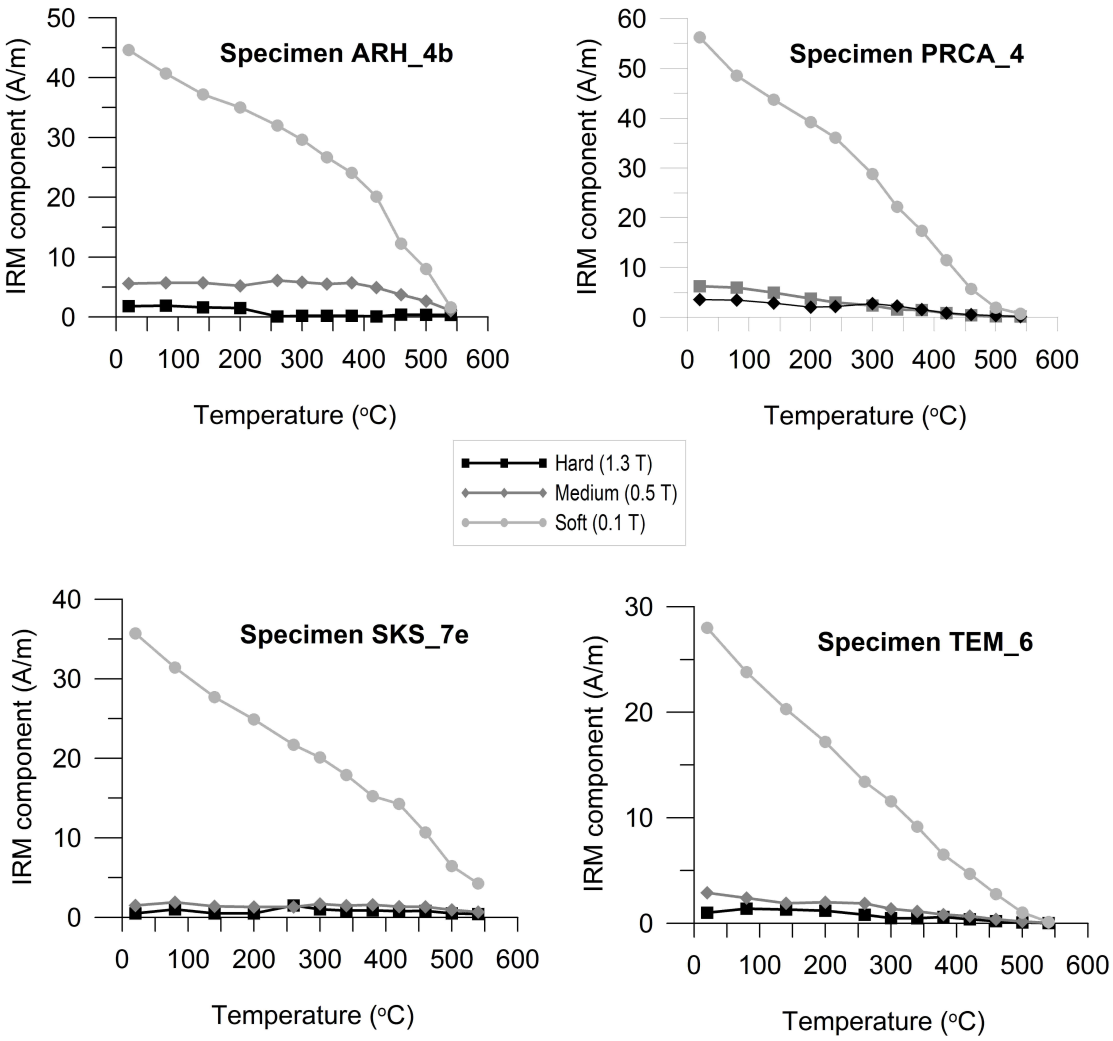
Specimen ARH_4b
IRM component (A/m)
Temperature (°C)
Specimen PRCA_4
IRM component (A/m)
Temperature (°C)
Hard (1.3 T)
Medium (0.5 T)
Soft (0.1 T)
Specimen SKS_7e
IRM component (A/m)
Temperature (°C)
Specimen TEM_6
IRM component (A/m)
Temperature (°C)

Fig. 4

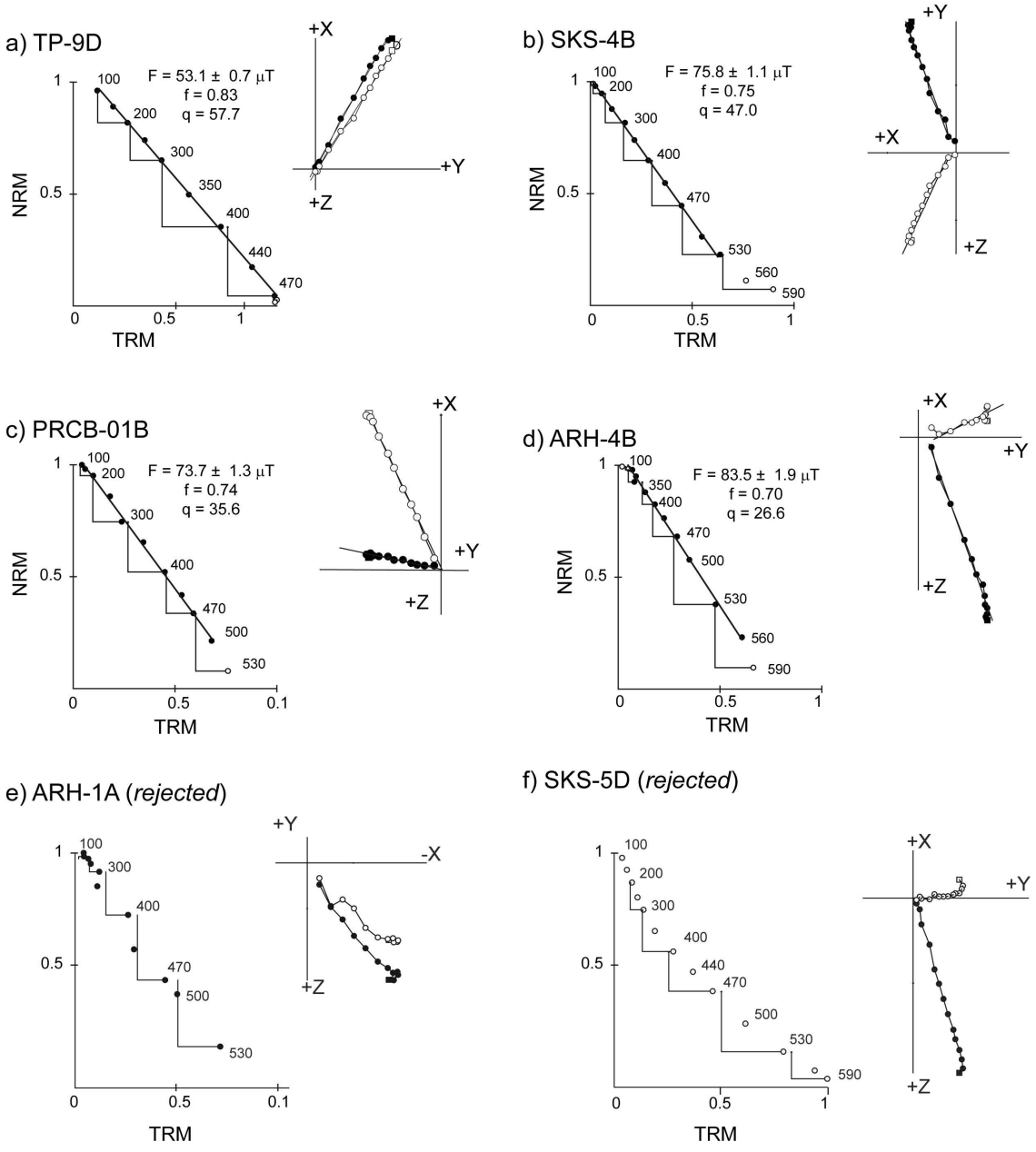
a) TP-9D
F = 53.1 ± 0.7 μT
f = 0.83
q = 57.7
NRM
TRM
+X
+Y
+Z
b) SKS-4B
F = 75.8 ± 1.1 μT
f = 0.75
q = 47.0
c) PRCB-01B
F = 73.7 ± 1.3 μT
f = 0.74
q = 35.6
d) ARH-4B
F = 83.5 ± 1.9 μT
f = 0.70
q = 26.6
e) ARH-1A (rejected)
-X
f) SKS-5D (rejected)

Fig. 5

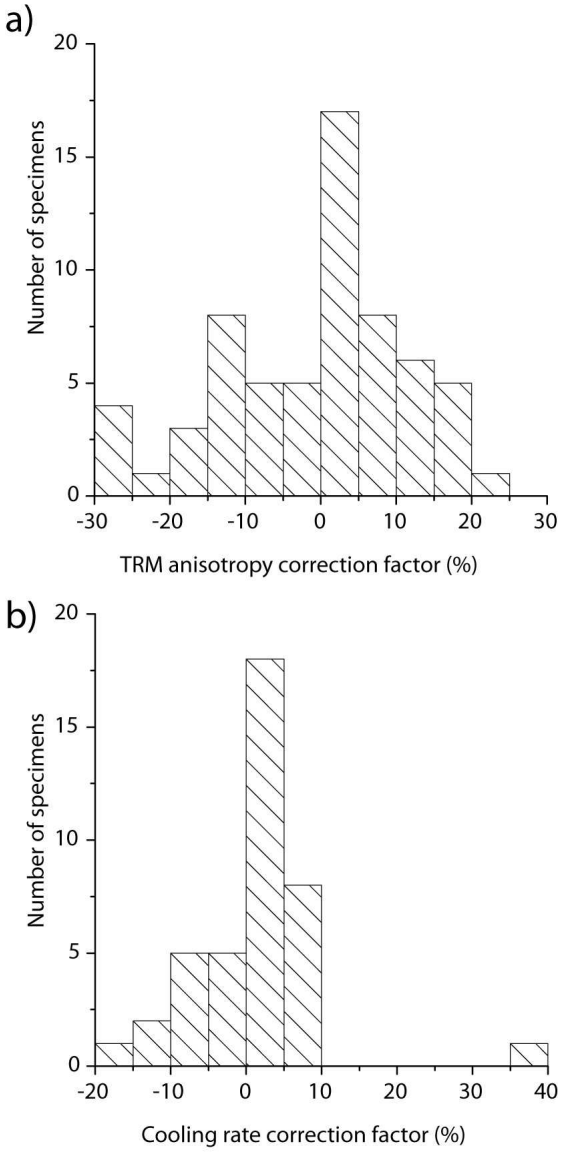
a)
Number of specimens
TRM anisotropy correction factor (%)
b)
Number of specimens
Cooling rate correction factor (%)

Fig. 6

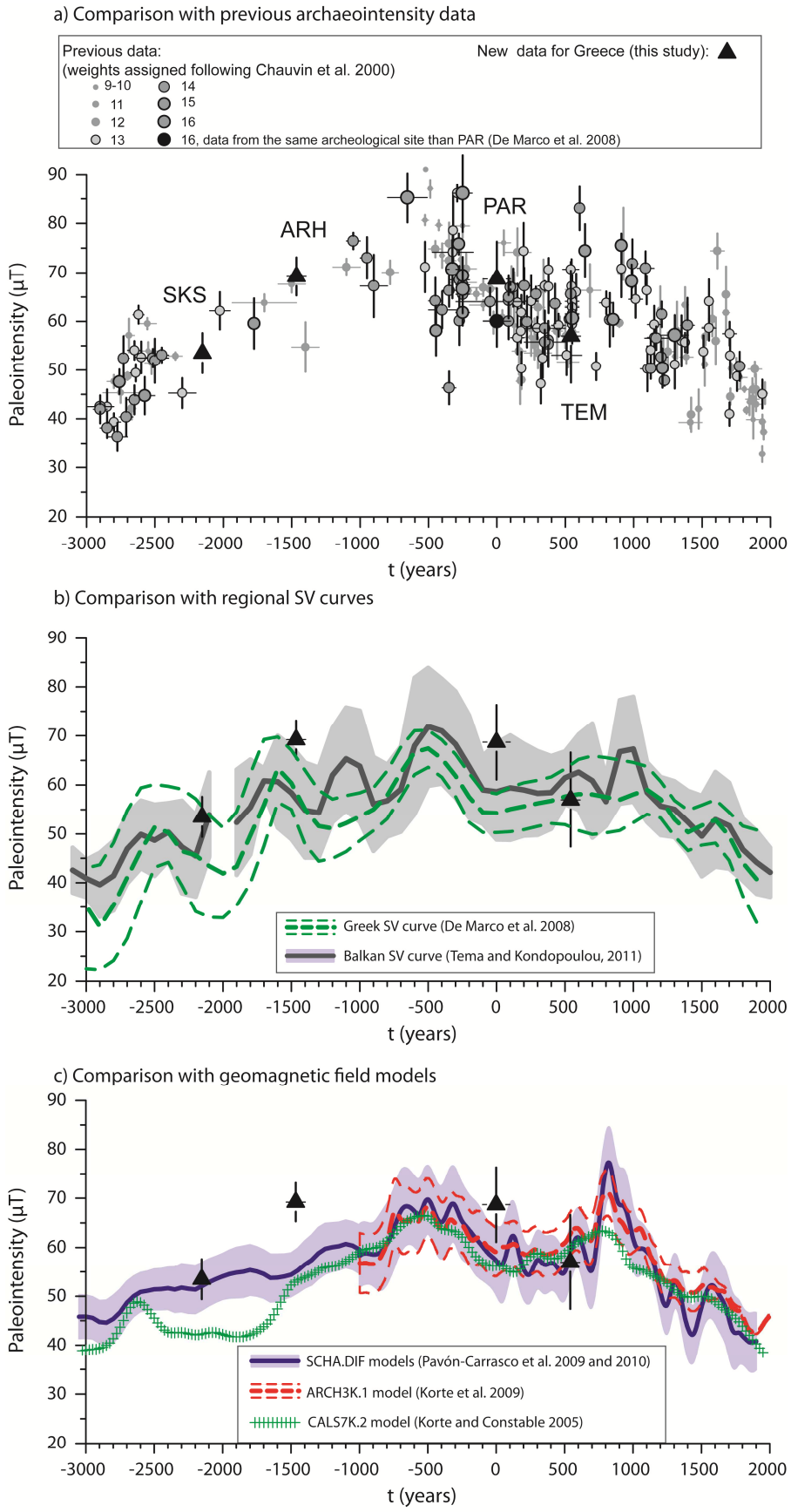
a) Comparison with previous archaeointensity data
Previous data:
(weights assigned following Chauvin et al. 2000)
9-10
11
12
13
14
15
16
16, data from the same archeological site than PAR (De Marco et al. 2008)
New data for Greece (this study):
SKS
ARH
PAR
TEM
Paleointensity (μT)
t (years)
b) Comparison with regional SV curves
Greek SV curve (De Marco et al. 2008)
Balkan SV curve (Tema and Kondopoulou, 2011)
c) Comparison with geomagnetic field models
SCHA.DIF models (Pavón-Carrasco et al. 2009 and 2010)
ARCH3K.1 model (Korte et al. 2009)
CALS7K.2 model (Korte and Constable 2005)

Fig. 7